


 Cite this: *RSC Adv.*, 2024, 14, 31320

# Green and recyclable catalyst based on chitosan/ CuFe<sub>2</sub>O<sub>4</sub> nanocomposite hydrogel for one-step synthesis of 1,2,3-triazoles†

 Fatemeh Ajormal,<sup>a</sup> Rahman Bikas,<sup>b</sup> Hossein Ghasemzadeh,<sup>\*b</sup>  
 Nader Noshiranzadeh<sup>c</sup> and Anna Kozakiewicz-Piekarz<sup>c</sup>

The scope of the heterogeneous catalysts has been greatly expanded in last few decades by the development of various catalysts. In this work a new chitosan-based nanocomposite hydrogel (CS/CuFe<sub>2</sub>O<sub>4</sub> NCH) was synthesized as a high-performance heterogeneous catalyst and then, it was utilized for the green synthesis of substituted 1,2,3-triazoles by a multi-component (azide-alkyne-epoxide) cycloaddition reaction. The synthesized nanocomposite hydrogel was investigated by using various instrumental analyses, including FT-IR, XRD, SEM, EDS, HRTEM, DLS, and TGA. The structure of one of the substituted 1,2,3-triazoles was studied by using single-crystal X-ray diffraction analysis. The nanocomposite hydrogel can be easily regenerate after the catalytic reaction. It can be reused frequently without considerable loss of activity. The high catalytic activity, straightforward reaction, easy recyclability, short reaction time, use of a green solvent, and the simple separation of catalyst are the main advantage of the current method, which offers both financial and environmental benefits.

 Received 2nd August 2024  
 Accepted 20th September 2024

DOI: 10.1039/d4ra05626d

[rsc.li/rsc-advances](https://rsc.li/rsc-advances)

## 1. Introduction

Green chemistry has received much attention in recent years, mostly for environmental and economic reasons. The replacement of petroleum-based materials with natural-source materials has become a significant need.<sup>1,2</sup> This demand increases when it comes to items that are related to human health, such as medical, pharmaceutical, and food products.<sup>3</sup> One important aspect of the green chemistry, that has received high attention, is the manufacture of the active green catalytic systems. Designing a safe, low-cost, and stable heterogeneous catalytic system based on natural products represents an effective strategy for preparing environmentally friendly catalytic systems.<sup>4,5</sup> Hydrogels are polymeric networks that can serve as water absorbents due to their hydrophilic nature.<sup>6,7</sup> Hydrogels can be synthesized using natural materials. Most of the natural based hydrogels can be considered as green materials. Hydrogels offer a broad range of applications due to their physico-chemical properties, such as excellent solvent compatibility,

and porous structure.<sup>8–11</sup> Hydrogels are also interesting and useful materials for preparing nanocomposites. A range of nanocomposites hydrogels have been prepared successfully.<sup>12</sup> They have been utilized in several fields, including biomedicine,<sup>13–15</sup> antibacterial studies,<sup>16,17</sup> water treatment,<sup>18,19</sup> drug delivery,<sup>20–22</sup> *etc.* The synthesis, applications, and various properties of the nanocomposite hydrogels have been reported by several review articles.<sup>23–25</sup> Nano-composite hydrogels have also been used as catalysts in various reactions, including C–C coupling,<sup>26,27</sup> reduction of organic materials,<sup>28–31</sup> and oxidation of alcohols.<sup>32</sup>

1,2,3-Triazoles are a class of nitrogen-rich heterocyclic compounds that are commonly used in several applications such as sensors,<sup>33</sup> herbicides,<sup>34</sup> fungicides,<sup>35–37</sup> corrosion-resistant agents,<sup>38</sup> solar cells and dyes,<sup>39</sup> and catalysis.<sup>40</sup> Due to various biological activities, including anti HIV,<sup>41,42</sup> anti bacterial,<sup>43</sup> and anti allergy<sup>44</sup> properties, they are also important compounds in the preparation of novel drugs and development their activities. Therefore, green, and effective synthesis of triazoles has attracted considerable attention in recent years.<sup>45,46</sup> Several techniques have been used for the synthesis of triazoles. The thermal cycloaddition reaction of azides with alkynes in the presence of copper catalysts is one the most interesting methods.<sup>47–50</sup> Although the primary approaches were based on the use of active Cu(I) species,<sup>51,52</sup> several works have reported the direct use of Cu(II) species as a catalyst for synthesis of triazoles.<sup>53,54</sup> In addition, β-hydroxy-1,2,3-triazoles has been synthesized by *in situ* ring opening of epoxide in the presence of sodium azide and an alkyne.<sup>55</sup> Several catalytic systems have

<sup>a</sup>Department of Chemistry, Faculty of Science, University of Zanjan, Zanjan, 45371-38791, Iran

<sup>b</sup>Department of Chemistry, Faculty of Science, Imam Khomeini International University, Qazvin, 34148-96818, Iran. E-mail: hoghasemzadeh@sci.ikiu.ac.ir; bikas@sci.ikiu.ac.ir

<sup>c</sup>Department of Biomedical and Polymer Chemistry, Faculty of Chemistry, Nicolaus Copernicus University in Torun, Torun, 87-100, Poland

 † Electronic supplementary information (ESI) available. CCDC 2264680. For ESI and crystallographic data in CIF or other electronic format see DOI: <https://doi.org/10.1039/d4ra05626d>


also been developed for the synthesis of 1,4-disubstituted-1,2,3-triazoles.<sup>56–59</sup> Several studies have been carried out to prepare green and reusable systems for the synthesis of triazoles.<sup>60–62</sup> Although a few works were reported about the synthesis of triazoles by use of nanocomposite hydrogels,<sup>63,64</sup> new catalytic systems based on the nanocomposite hydrogels can be developed for green synthesis of triazoles under mild conditions.

In this work, a nanocomposite hydrogel was synthesized based on the chitosan, formaldehyde,  $\text{Cu}(\text{NO}_3)_2 \cdot 3\text{H}_2\text{O}$ , and  $\text{Fe}(\text{NO}_3)_3 \cdot 9\text{H}_2\text{O}$  and used successfully as an effective catalyst for the green synthesis of 1,2,3-triazoles by an azide-epoxide-alkyne cycloaddition reaction. Chitosan is a valuable starting compound for the synthesis of hydrogels due to its unique properties, including non-toxicity, hydrophilic nature, renewability, and chelating properties.<sup>65</sup> The obtained nanocomposite hydrogel was characterized by several instrumental methods. The results demonstrated that the catalytic system has great stability and recycling efficiency for the production of triazole in aqueous solution. The synthesized catalytic system can be considered as a low-cost green catalyst for the synthesis of triazoles.

## 2. Experimental

### 2.1 Materials

Formaldehyde, sodium hydroxide (NaOH), ferric nitrate ( $\text{Fe}(\text{NO}_3)_3 \cdot 9\text{H}_2\text{O}$ ), copper(II) nitrate ( $\text{Cu}(\text{NO}_3)_2 \cdot 3\text{H}_2\text{O}$ ), sodium azide, propylene oxide, phenylacetylene, 2-methylbut-3-butyn-2-ol, 1-ethynylcyclohexanol, 2-(phenoxy)methyl oxirane and solvents were purchased from Sigma-Aldrich Co. High molecular weight chitosan (CS), with deacetylation degree (DD) of 85% was prepared from Sigma-Aldrich Co. All chemicals were used without further purification. Distilled water (DW) was also used in all experiments.

### 2.2 Preparation of hydrogel and nanocomposite hydrogel CS/CuFe<sub>2</sub>O<sub>4</sub>

The hydrogel was prepared according to the reported procedure.<sup>66</sup> To create the chitosan hydrogel, 0.4 g of chitosan was poured to 40 mL distilled water, followed by addition of 2.0 mL acetic acid. The mixture was stirred for 10 min at 80 °C to achieve a homogenous solution. Then, formaldehyde (2.0 mL) was added to the solution. The solution was stirred for 10 min at 80 °C. After the formation of low-strength hydrogels, the product was permitted to reach to room temperature.  $\text{CuFe}_2\text{O}_4$  nanoparticles were prepared within the hydrogel by *in situ* coprecipitation of copper(II) nitrate and iron(III) nitrate in aqueous solution. First,  $\text{Cu}(\text{NO}_3)_2 \cdot 3\text{H}_2\text{O}$  (2.0 mmol, 0.49 g), and  $\text{Fe}(\text{NO}_3)_3 \cdot 9\text{H}_2\text{O}$  (4.0 mmol, 0.82 g) were dissolved in 5.0 mL deionized water in two different flasks. After full dissolving, the solutions were combined and poured in a 20 mL flask and the hydrogel was placed in the solution. The hydrogel remained in the solution at room temperature for 24 h. Then, the hydrogel was treated dropwise with NaOH solution (20.0 mL, 0.04 M) for 30 min. Then, the mixture was heated to 45–50 °C for 30 min. After cooling, the gel containing nanoparticles was filtered and

rinsed with 200 mL of deionized water. The nanocomposite hydrogel ( $\text{CS}/\text{CuFe}_2\text{O}_4$ ) was then placed in 100 mL of ethanol and stirred at room temperature overnight to remove the water. The nanocomposite hydrogel was then filtered, and the sample was dried at 40 °C in a vacuum condition for 24 h.

### 2.3 Hydrogel characterization

Fourier transform infrared (FT-IR) spectra were obtained using KBr pellets on a Bruker Tensor 27 spectrophotometer. HR-TEM (FEI TECNAI F20TEM) and dynamic light scattering (DLS) by VASCO Cordouan technologies were used to determine the size of the nanoparticles. The  $\text{CS}/\text{CuFe}_2\text{O}_4$  nanocomposite hydrogel was dispersed in distilled water by an ultrasonic homogenizer for 20 min. The morphology of the nanocomposite hydrogel was investigated by FE-SEM (TESCAN MIRA3) after freeze-drying. X-ray diffraction (XRD) pattern was studied using an XRD Philips PW1730 diffractometer with  $\text{Cu-K}\alpha$  radiation in the scan range of  $2\theta = 10\text{--}80^\circ$  at ambient temperature.

### 2.4 Water absorbency measurement

The water absorbency of the hydrogel was examined in distilled water at ambient temperature and gentle stirring (150 rpm). In brief, 3 samples with a certain amount of dry hydrogel (0.2 g) were weighed carefully and placed in distilled water. At

Table 1 Structure refinement and crystal data for compound T2

Compound	T2
CCDC No	2264680
Net formula	$\text{C}_{13}\text{H}_{17}\text{N}_3\text{O}_2$
$M_r/\text{g mol}^{-1}$	247.29
Crystal size/mm	$0.58 \times 0.12 \times 0.10$
$T/\text{K}$	293
Radiation	Mo ( $0.71073 \text{ \AA}$ )
Crystal system	Monoclinic
Crystal shape, color	Needle/colorless
Space group	$P2_1/c$
$a/\text{\AA}$	8.6436 (5)
$b/\text{\AA}$	18.9145 (12)
$c/\text{\AA}$	8.3234 (5)
$\beta/^\circ$	99.035 (6)
$V/\text{\AA}^{-3}$	1343.90 (14)
$Z$	4
Calc. density/ $\text{g cm}^{-3}$	1.222
$\mu/\text{mm}^{-1}$	0.09
$F(000)$	528
$\theta$ range/ $^\circ$	2.2–28.3
$h$	–11 → 11
$k$	–24 → 24
$l$	–4 → 10
$R_{\text{int}}$	0.054
$R1$	0.0602
$wR2$	0.1184
$S$	1.041
Abs. correction	Multi-scan
Measured reflections	8914
Independent reflections	3043
Parameters	163
Restraints	0
Largest diff. peak and hole	0.418/–0.227



specified time points, the hydrogels were removed from the water and was drained carefully and weighed again. The swelling was calculated by the eqn (1).

$$\text{Swelling}(\%) = \frac{W_t - W_0}{W_0} \quad (1)$$

where  $W_t$  and  $W_0$  are the weights of the hydrogel after and before the swelling, respectively.

### 2.5 Determination of gel content

To assess the gel content, three dry gel samples were carefully weighed before being submerged in the swelling medium. Then, specified amounts of the dry hydrogel samples ( $W_b$ ) were immersed in deionized water in 250 mL flasks for 24 h. The swollen hydrogels were then cleaned and filtered repeatedly. The swollen samples were immersed in ethanol to eliminate water and then being dried at 50 °C in an oven for 24 h ( $W_a$ ). The gel content was estimated using eqn (2).

$$\text{Gel}(\%) = \frac{W_a}{W_b} \times 100 \quad (2)$$

### 2.6 General experimental procedure for the synthesis of 1,2,3-triazoles

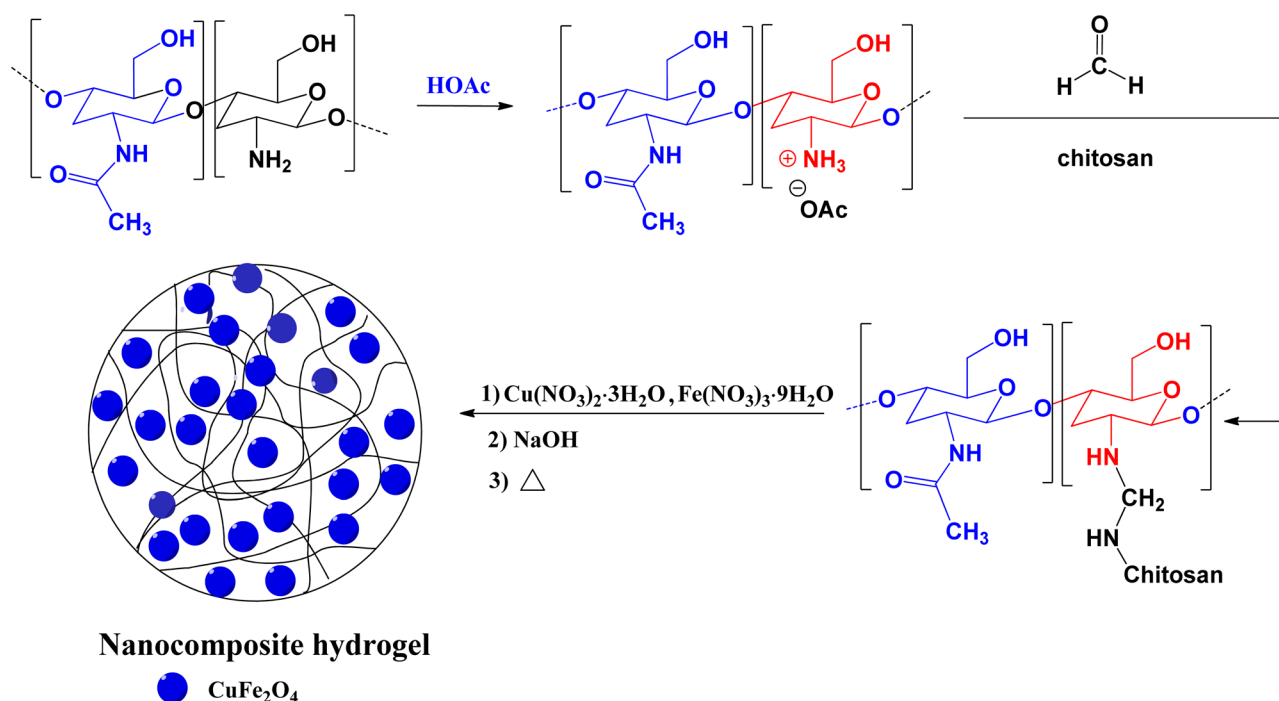
A glass vial was filled with 1.0 mmol of phenylacetylene, 1.5 mmol of sodium azide, 1.0 mmol of epoxide, 10–60 mg of CS/CuFe<sub>2</sub>O<sub>4</sub> nanocomposite hydrogel as a catalyst, and 4.0 mL of distilled water. The heterogeneous reaction mixture was then stirred (250 rpm) for 12 h at room temperature. To investigate the development of the reaction, thin-layer chromatography

(TLC) was used. After the starting materials were completely disappeared, 5.0 mL ethyl acetate was added into the reaction medium and stirred for 10 min before separating the nanocomposite hydrogel. This process was repeated three times. The extracted products were purified by column chromatography using silica gel and a mixture of ethyl acetate/hexane. Spectroscopic methods (FT-IR, <sup>1</sup>H NMR, and <sup>13</sup>C NMR) were applied to determine the structures of the products. Single crystal X-ray analysis was used to determine the crystal structure of one of the products (T2). The analysis of single crystal X-ray and structure refinements are present in the ESI†. A list of important crystallographic parameters related to single crystal X-ray analysis and refinement is depicted in Table 1.

## 3. Results and discussion

### 3.1 Hydrogel synthesis and characterization

The hydrogel matrix consists of many micro and nano pores that can act as the nanoreactors. The nanoreactors can be utilized for production of the nanoparticles. The nanocomposite hydrogel was prepared by the reaction of chitosan and formaldehyde followed by treatment with Cu(NO<sub>3</sub>)<sub>2</sub>·3H<sub>2</sub>O and Fe(NO<sub>3</sub>)<sub>3</sub>·9H<sub>2</sub>O salts. Chitosan was cross-linked with formaldehyde by condensation of primary amines of chitosan with formaldehyde. Copper(II) and iron(III) ions also have a stabilizing role in hydrogel strength through ionic cross-linking. The cross-linking reaction and formation of the nanocomposite hydrogel are shown in Scheme 1. The nanocomposite hydrogel was synthesized by coprecipitation of copper(II) nitrate and iron(III) nitrate within the hydrogel in an alkaline aqueous solution. The structure of the CS/CuFe<sub>2</sub>O<sub>4</sub> nanocomposite hydrogel was confirmed by FT-IR, TGA, DLS, FE-SEM, HR-TEM, EDS, and XRD analyses.



Scheme 1 Schematic illustration for the formation of CS/CuFe<sub>2</sub>O<sub>4</sub> nanocomposite hydrogel.



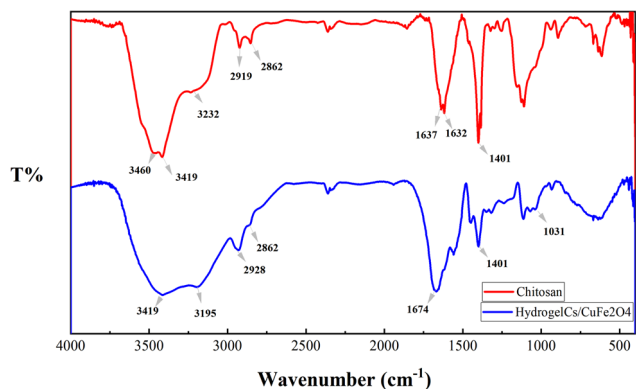


Fig. 1 FT-IR spectra of chitosan (red line) and nanocomposite hydrogel CS/CuFe<sub>2</sub>O<sub>4</sub> (blue line).

The FT-IR spectra of the pure chitosan and CS/CuFe<sub>2</sub>O<sub>4</sub> nanocomposite hydrogel are shown in Fig. 1. The spectrum of hydrogel indicates the typical bands of the starting material

with some discrepancies. The broad band with a center at about 3420 cm<sup>-1</sup> is related to the stretching of the hydroxyl groups (O–H).<sup>67</sup> The spectrum displays two well-defined peaks at about 3400 cm<sup>-1</sup> which are also observed in chitosan. These peaks are somewhat weakened in the hydrogel sample, which is due to the reaction of the free amino groups with formaldehyde. In the spectrum of the hydrogel the remaining amide group of chitosan shows peak at around 1632–1637 cm<sup>-1</sup>,<sup>68</sup> whereas the absorption band is shifted to 1674 cm<sup>-1</sup> in nanocomposite hydrogel. The presence of CuFe<sub>2</sub>O<sub>4</sub> in the nanocomposite hydrogel causes a shift in the peak. The change in absorption bands at about 1031–1171 cm<sup>-1</sup> in the spectrum of hydrogel are due to the formation of new C–N bonds that are formed by reaction between amino groups and formaldehyde.<sup>69</sup> These peaks are the result of asymmetric stretching of C–O–C and C–N–C units in the structure of the nanocomposite hydrogel.

To investigate the presence of CuFe<sub>2</sub>O<sub>4</sub> in the nanocomposite hydrogel, XRD analysis was performed at room temperature (Fig. 2). The XRD pattern demonstrated reflection

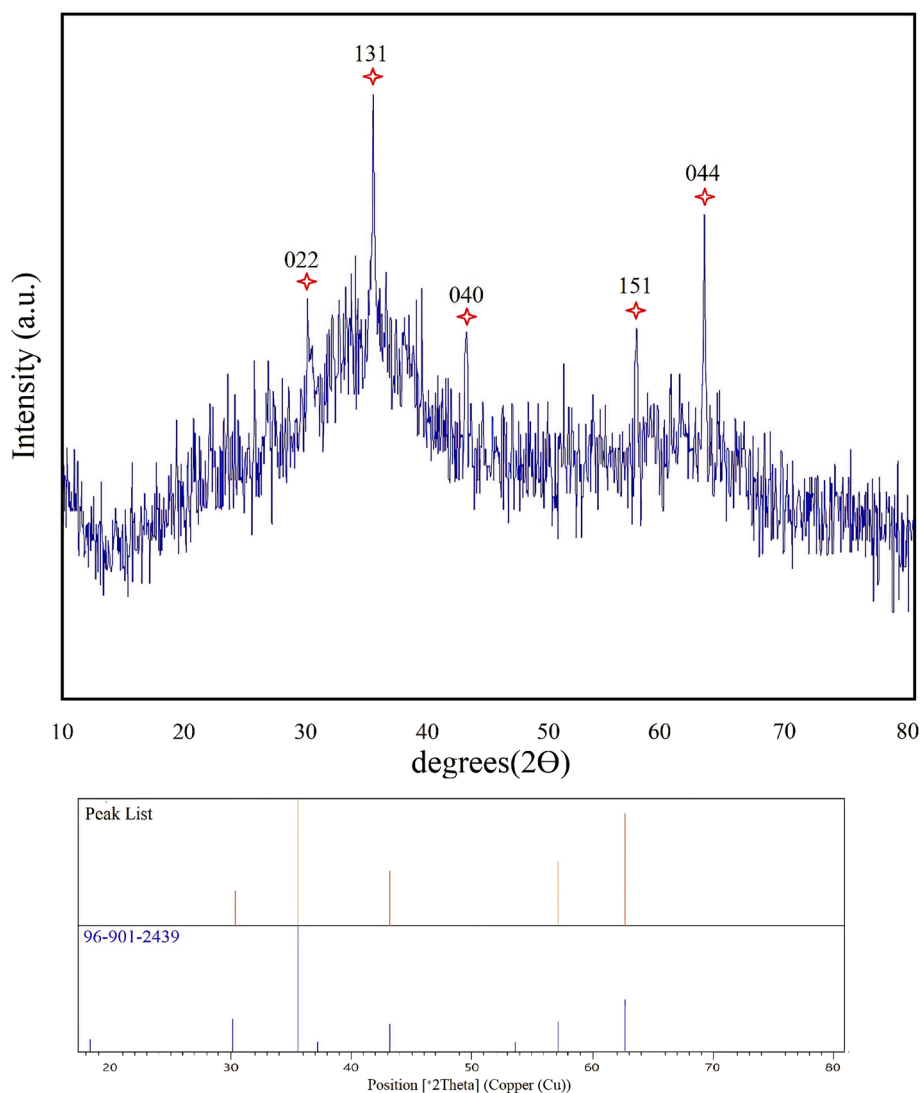


Fig. 2 XRD pattern of nanocomposite hydrogel CS/CuFe<sub>2</sub>O<sub>4</sub>.



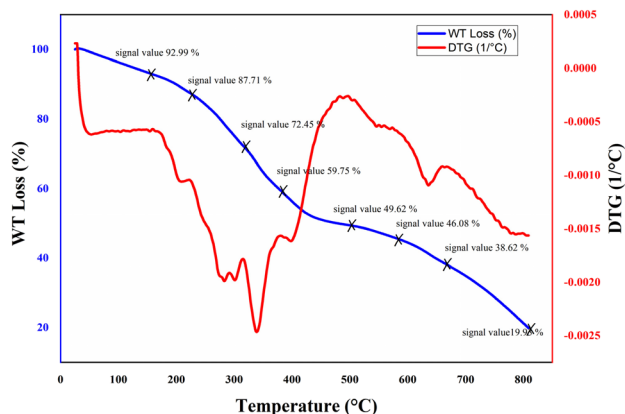


Fig. 3 TGA analysis of the CS/CuFe<sub>2</sub>O<sub>4</sub> nanocomposite hydrogel.

peaks at  $2\theta = 30.32, 35.54, 43.18, 57.13,$  and  $62.73^\circ$  which are well in line with the standard XRD pattern of CuFe<sub>2</sub>O<sub>4</sub> (96-901-2439). These results show the presence of CuFe<sub>2</sub>O<sub>4</sub> in the composition of the obtained nanocomposite hydrogel. Also, the crystal size of CuFe<sub>2</sub>O<sub>4</sub> nanoparticles was quantitatively calculated using the Scherrer equation, which was estimated to be about 46 nm.

To investigate the thermal behavior of the nanocomposite hydrogel, thermogravimetric analysis (TGA) was conducted in the range of 25–800 °C (Fig. 3). TGA thermogram showed ~7% of weight loss at 150 °C which is related to the removal of moisture from the structure. A gradual weight loss is seen at temperatures around 250 to 580 °C which is attributed to the degradation of the major backbone of the hydrogel. During this

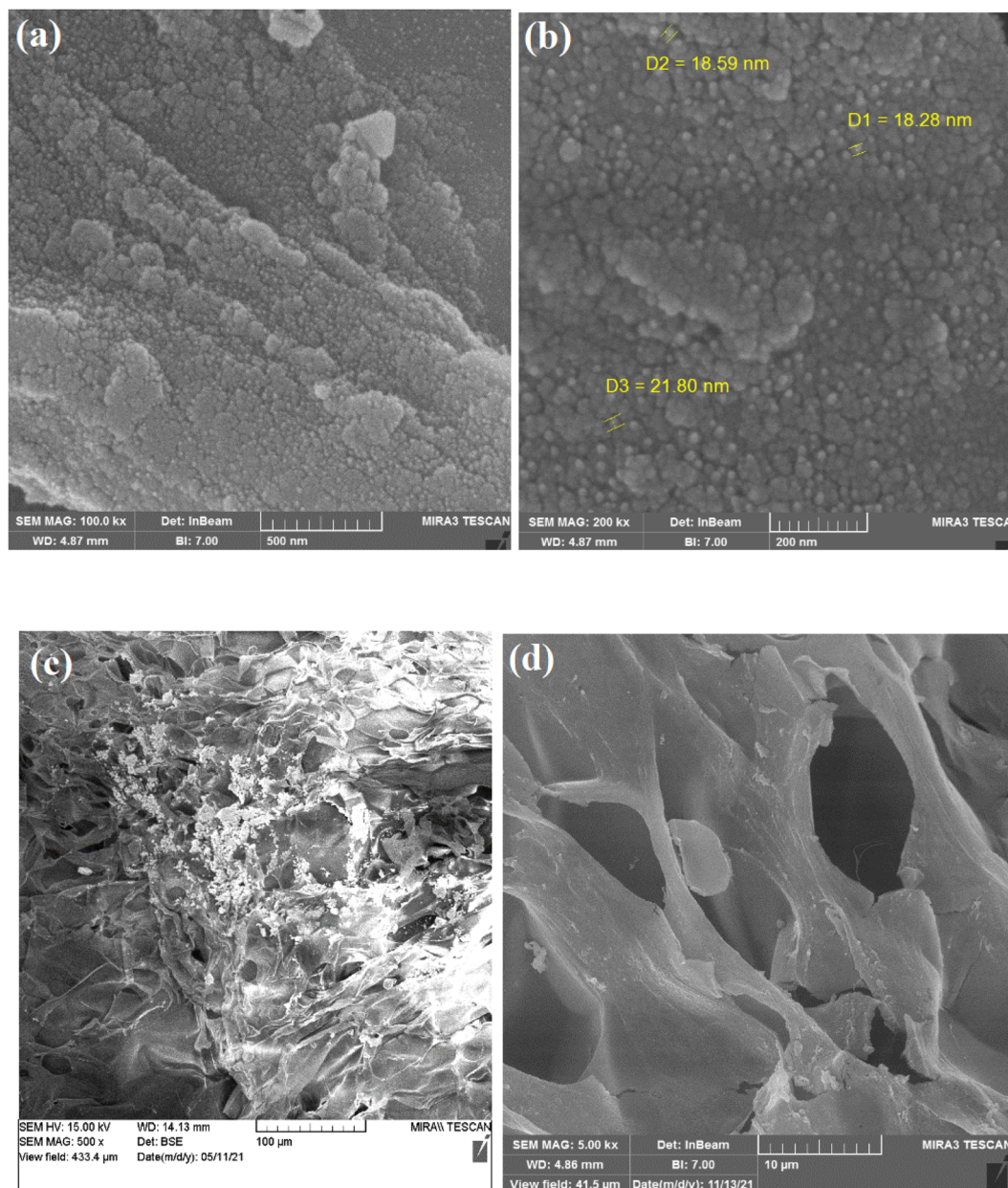


Fig. 4 SEM analysis of the nanocomposite hydrogel catalyst (CS/CuFe<sub>2</sub>O<sub>4</sub>) with magnification of (a) 100 000 $\times$ , (b) 200 000 $\times$ , (c) 500 $\times$  and (d) 5000 $\times$ .



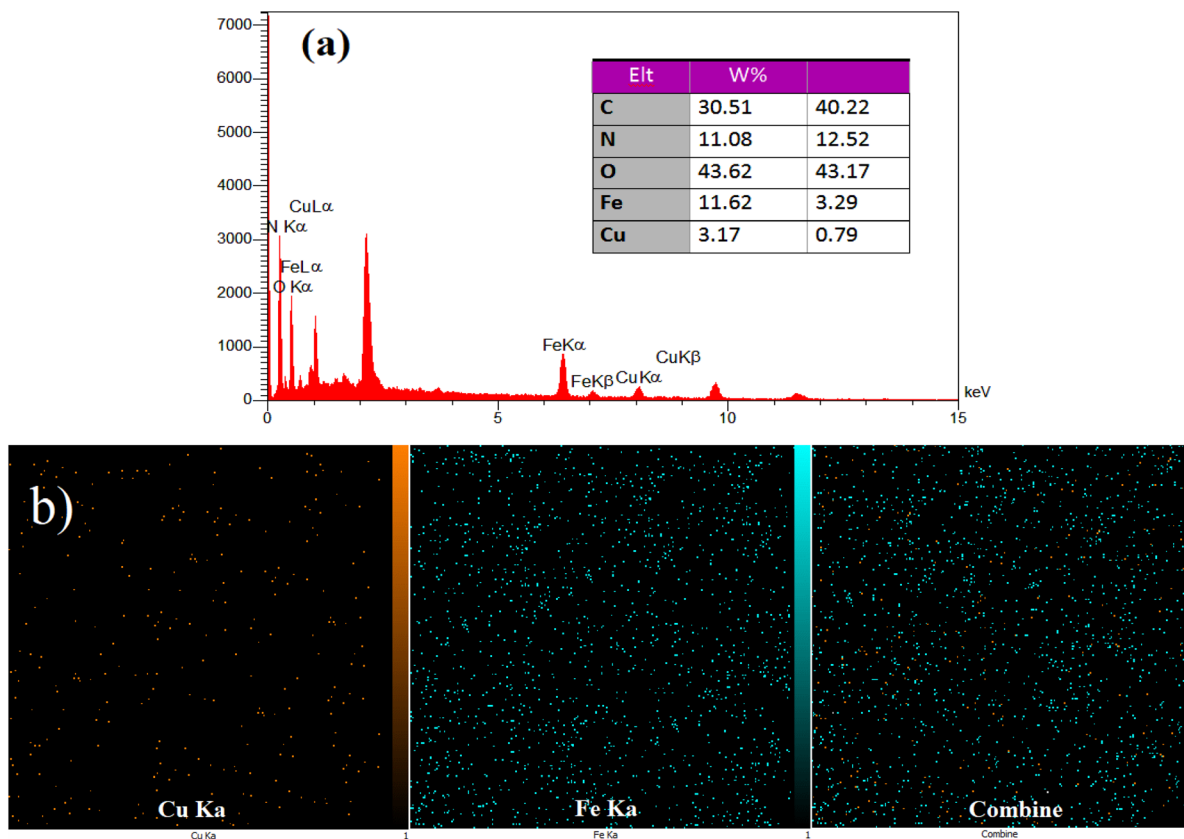


Fig. 5 (a) EDS and (b) X-ray mapping of the CS/CuFe<sub>2</sub>O<sub>4</sub> nanocomposite hydrogel catalyst.

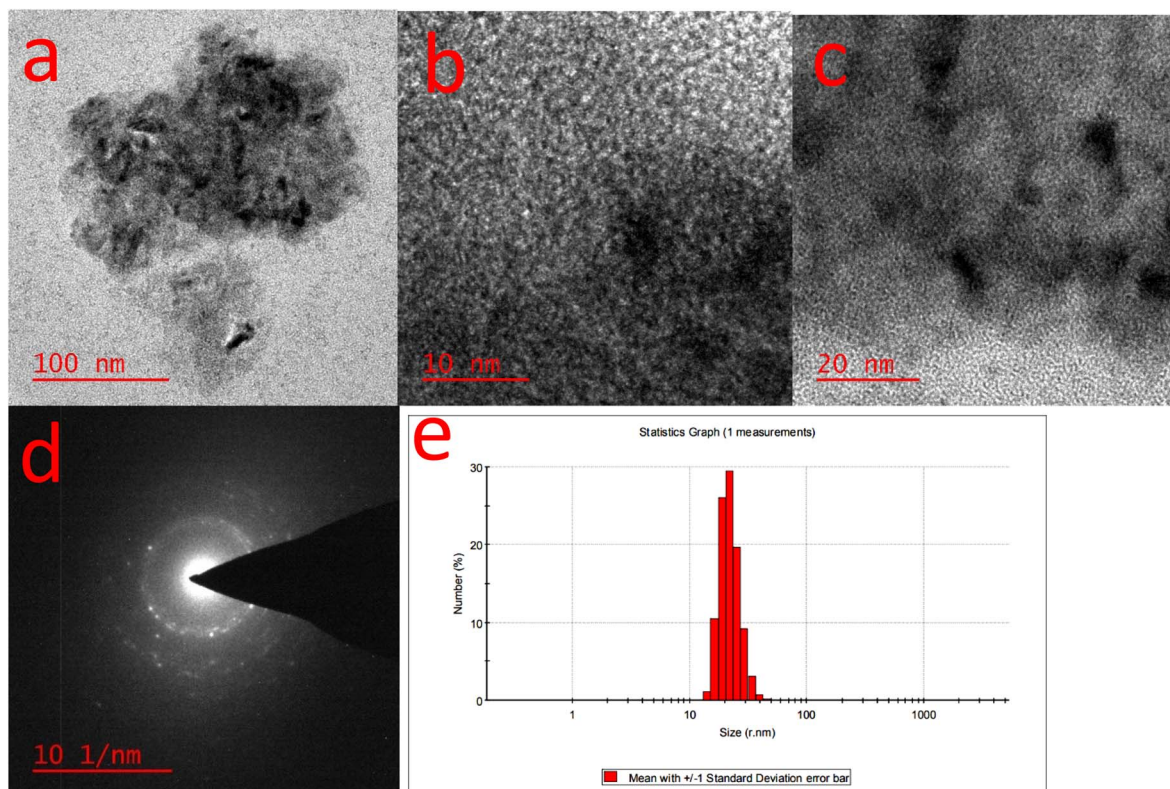


Fig. 6 CuFe<sub>2</sub>O<sub>4</sub> particle characterization by HR-TEM. HR-TEM image of the CuFe<sub>2</sub>O<sub>4</sub> nanocomposite hydrogel catalyst, with various magnification (a–c), SAED pattern of the CuFe<sub>2</sub>O<sub>4</sub> nanocomposite hydrogel (d), and particle size distribution obtained by DLS analysis (e).



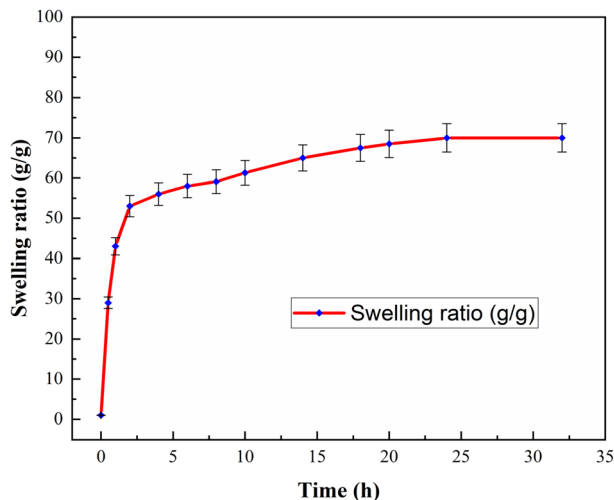


Fig. 7 Swelling rate of CS/CuFe<sub>2</sub>O<sub>4</sub> nanocomposite hydrogel at different times at 25 °C.

Table 2 The effect of the amount of catalyst on the time of reaction and yield in the synthesis of 1,2,3-triazole (T1)

Entry	Catalyst (mg)	Time (h)	Yield (%)
1	0	48	0
2	10	21	48
3	20	15	76
4	30	11	94
5	40	8	96
6	60	7	95

step, the polymer chains of the nanocomposite hydrogel are broken down into smaller pieces. Finally, when the temperature has reached about 750 °C, the residue ratio of the nanocomposite hydrogel was around 20%. This behavior indicates the remarkable heat stability of the synthesized nanocomposite hydrogel.

The field-emission scanning electron microscopy image (FE-SEM) technique was applied to study the surface morphology of the nanocomposite hydrogel. The nanocomposite hydrogel shows a rough and porous structure with a high number of holes. The CuFe<sub>2</sub>O<sub>4</sub> nanoparticles with a pretty regular spherical shape are present on the surface of the catalyst, as shown in Fig. 4.

EDS and X-ray mapping analysis were performed on the produced heterogeneous catalyst (see Fig. 5). The EDS spectrum (Fig. 5a) reveals the presence of copper (Cu) and iron (Fe) elements in the nanocomposite at percentages of 3.17 wt% and 11.62 wt%, respectively. In addition, the carbon (C, 30.51 wt%), oxygen (O, 43.62 wt%) and nitrogen (N, 11.08 wt%) are present in the composition of the synthesized catalyst which confirms the successful synthesis of nanocomposite hydrogel. EDS mapping was used to assess the distribution of Fe and Cu ions on the surface of the nanocomposite hydrogel. The Fe and Cu elements are uniformly distributed throughout the nanocomposite hydrogel (Fig. 5b).

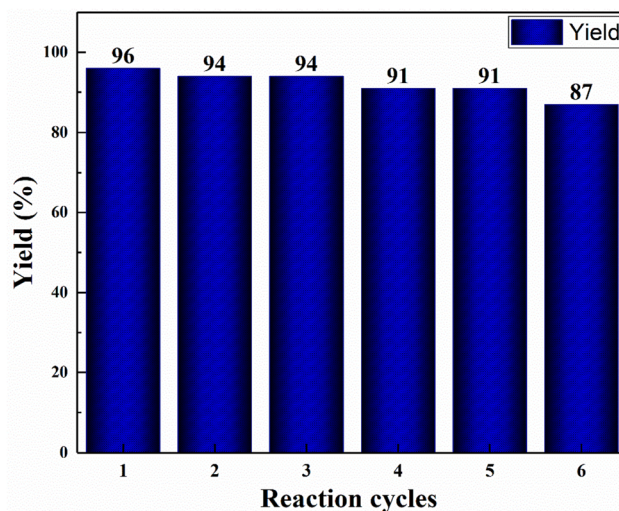


Fig. 8 1,2,3-Triazole (T1) yield after each sequential reaction cycles.

The CuFe<sub>2</sub>O<sub>4</sub> nanoparticles were studied by high-resolution transmission electron microscopy (HR-TEM) and DLS techniques. HR-TEM images are shown in Fig. 6 which reveal that the CuFe<sub>2</sub>O<sub>4</sub> nanoparticles are present in the nanocomposite hydrogel with the size of about 5 to 20 nm. DLS analyses of the nanocomposite hydrogel show the hydrodynamic diameters of the nanoparticles with a particle size of about 18–30 nm, which can be confirmed by TEM. As expected, the size of CS/CuFe<sub>2</sub>O<sub>4</sub> nanoparticles obtained from DLS analysis is higher than those obtained from TEM (Fig. 6).

### 3.2 Swelling rate and gel content

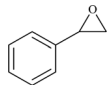
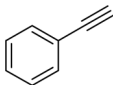
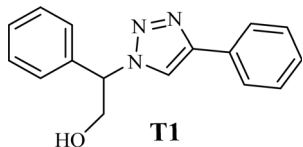
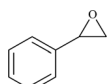
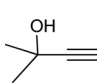
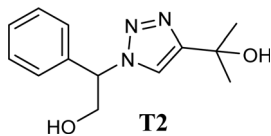
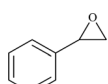
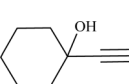
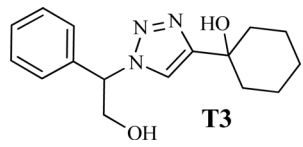
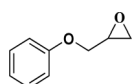
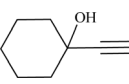
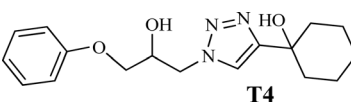
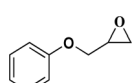
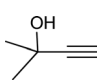
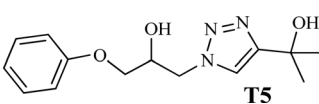
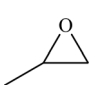
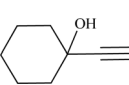
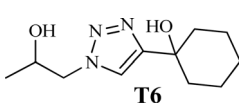
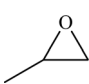
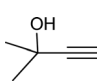
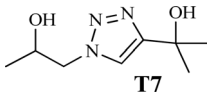
The swelling rate is an essential property of the hydrogels. The swelling behaviors of three samples of the nanocomposite hydrogels were studied at 25 °C in distilled water for 32 h. The averages of the swelling ratios were determined for the samples under the same circumstances and the results are shown in Fig. 7. It was found that the swelling rate of the nanocomposite hydrogels is sharply increased in the first two hours. Then, the rate of swelling showed a small change with time. The gel content of the nanocomposite hydrogel was also obtained 68.0%.

### 3.3 Catalytic activity

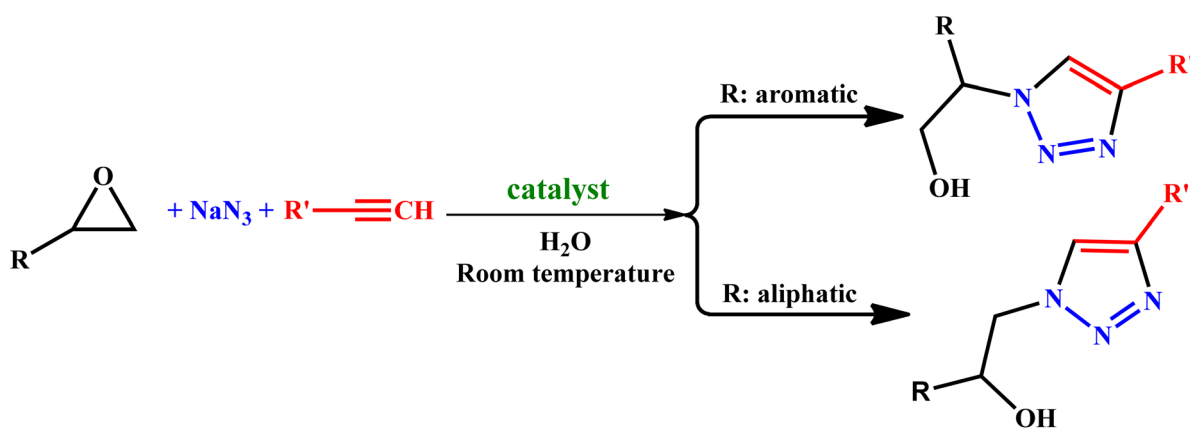
The catalytic ability of the CS/CuFe<sub>2</sub>O<sub>4</sub> nanocomposite hydrogel was investigated in the synthesis of 1,2,3-triazoles in an aqueous solution at ambient temperature. As a model reaction, a combination of phenylacetylene, styrene epoxide, and sodium azide was selected. A specified amount of the synthesized CS/CuFe<sub>2</sub>O<sub>4</sub> nanocomposite hydrogel was put in 4.0 mL of distilled water and shaken for 20 min. The reactive materials were poured in a reaction flask containing the catalyst and continuously stirred at 250 rpm. Thin-layer chromatography (TLC) was performed to track the course of the reaction. The optimization of the amount of the catalyst was carried out in the range of 10–60 mg and the results are collected in Table 2. The results



Table 3 The yields of the 1,2,3-triazoles synthesized using the nanocomposite hydrogel CS/CuFe<sub>2</sub>O<sub>4</sub> as a heterogeneous catalyst<sup>a</sup>

Entry	Epoxide	Alkyne	Product	Time (h)	Yield (%)	Selectivity (%)
1			 <b>T1</b>	8	96	>99
2			 <b>T2</b>	12	92	98
3			 <b>T3</b>	12	87	98
4			 <b>T4</b>	12	79	92
5			 <b>T5</b>	12	82	94
6			 <b>T6</b>	12	68	89
7			 <b>T7</b>	12	73	91

<sup>a</sup> Reaction condition: phenyl epoxy (1.0 mmol), alkynes (1.0 mmol), azide (1.5 mmol), nanocomposite hydrogel (40 mg of CuFe<sub>2</sub>O<sub>4</sub> nanocomposite hydrogel) and 4.0 mL of H<sub>2</sub>O at room temperature and air atmosphere.

Scheme 2 Synthesis of 1,2,3-triazoles using the CuFe<sub>2</sub>O<sub>4</sub> nanocomposite hydrogel as a heterogeneous catalyst.

demonstrate that an increase in the amount of catalyst led to a decrease in reaction time, which indicates that the catalyst possess a substantial effect on the rate of the reaction. The optimum amount of the catalyst was 40 mg for the production

of 2-phenyl-2-(4-phenyl-1H-1,2,3-triazol-1-yl)ethan-1-ol with 96% yield at ambient temperature after 8 h. In the same conditions but without using catalyst, the reaction was not preceded even after 48 h.





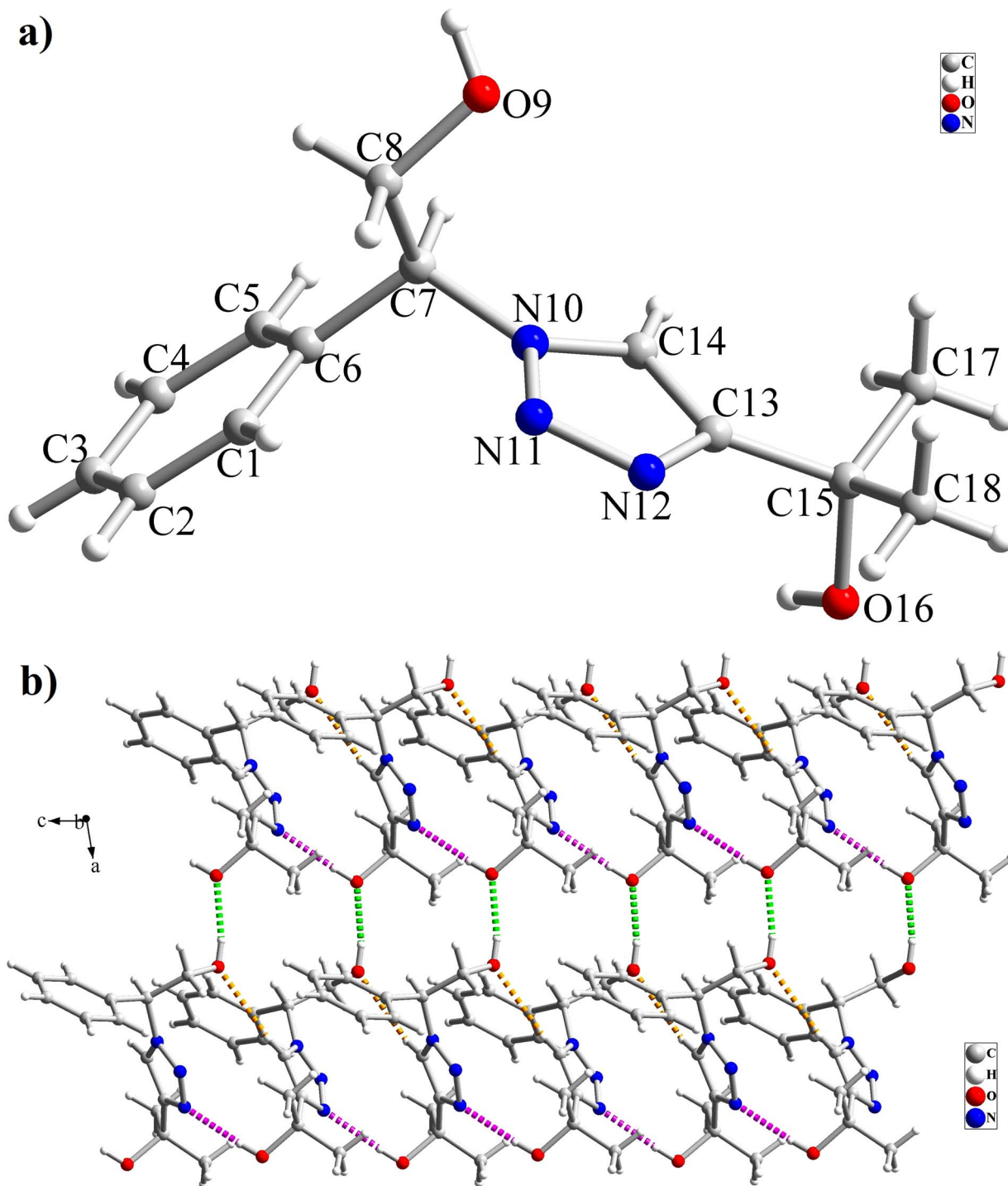


Fig. 9 (a) Crystal structure of T2; (b) interactions in the structure of T2 are shown as green (O–H···O), pink (O–H···N) and orange (C–H···O) dashed lines.

To reduce the manufacturing costs, recycling of catalysts is an important factor. Therefore, reusability of the nanocomposite hydrogel catalyst was investigated. When the reaction was completed, 5.0 mL of ethyl acetate was poured to the reaction medium and then stirred for 3 min to separate the product from the catalyst. The catalyst was then removed from the reaction mixture, rinsed with distilled water, and used again

in the same reaction. Six successive reactions were carried out with the nanocomposite hydrogel (Fig. 8). The catalyst remained stable even after six recoveries.

To examine the limitations of the reaction, a variety of derivatives of 1,2,3-triazole were produced by reaction of sodium azide with various epoxide and acetylenes (Table 3). High conversions (68–96%) were observed for all of these



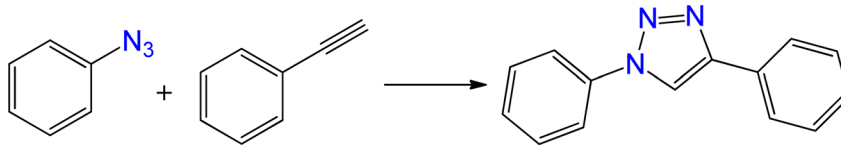
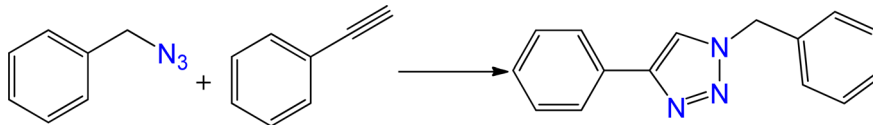
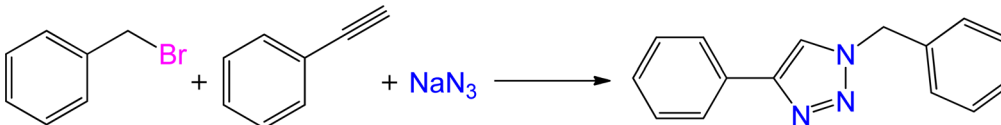
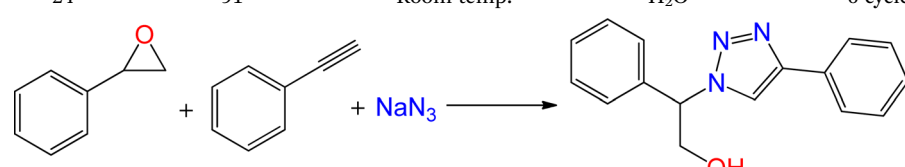
reactions, indicating the high catalytic activity of the CS/CuFe<sub>2</sub>O<sub>4</sub> nanocomposite hydrogel for the synthesis of the triazoles. However, the reaction with aliphatic alkynes (2-methylbut-3-yn-2-ol, 1-methyl-2-cyclohexen-1-ol) was slower than aromatic alkyne (phenylacetylene), indicating the importance of the group attached to the alkynes in this catalytic reaction. These groups have also a considerable effect on the ring opening reaction (see Scheme 2), which has been discussed in detail in our previous reports.<sup>70</sup>

The high purity products were obtained by recrystallization of the samples in methanol or ethanol solvents. All triazole derivatives were characterized by NMR and FT-IR spectroscopic methods after extraction and purification processes. In order to have stronger evidence about the formation of triazoles, the crystal structure of **T2** was further studied using single crystal X-ray analysis. We have previously reported the crystal structure of this compound<sup>71</sup> but, the primary results of the new data collection of the obtained crystals from methanol solvent indicated that the new crystals have different unit cell parameters than the previous one. After data collection and refinement processes, it was found that similar to the previous one<sup>71</sup> the obtained crystals are crystallized in *P2<sub>1</sub>/c* space group but, it is a new polymorph of the compound. Although the product is the

same as the previous, the new crystals have completely different intermolecular interactions which are consistent with the formation of a new crystal system. This situation is mainly related to the solvent that is used in the crystallization process. The structure of **T2** is illustrated in Fig. 9a. The interactions of the crystal structure are shown in Fig. 9b. The important crystallographic data for **T2** are shown in Table 1. The bond angles and bond lengths are also listed in Table S1.† The crystal structure of **T2** showed that the formation of triazole was carried out by the ring-opening reaction of the epoxide from the more substituted position. In the structure of **T2**, two aromatic rings including phenyl and triazole are observed with an angle of 112.43° relative to each other. The intermolecular hydrogen bonds are demonstrated in Fig. 9b, which are formed by two alcoholic OH groups. In addition, C–H···π interactions are also present which are shown in Fig. 9b and S1.†

To demonstrate the ability of the catalyst, a comparison was made compared with those reported in the literature (see Table S3†).<sup>70–74</sup> As indicated, the reaction times are comparable or slightly higher than that of the previous reports. Although the activity of the CuFe<sub>2</sub>O<sub>4</sub> nanocomposite hydrogel catalyst is relatively lower than the corresponding homogeneous systems.<sup>53,70,71</sup> The catalytic system exhibits great stability,

**Table 4** Comparing the catalytic performance of chitosan/CuFe<sub>2</sub>O<sub>4</sub> nanocomposite hydrogel with various catalysts in the synthesis of 1,2,3-triazoles

Catalyst	Time (h)	Yield (%)	Temperature (°C)	Solvent	Reusability	Ref.
						
Cs/PVA-CuNP	6	92	50	<i>t</i> BuOH/H <sub>2</sub> O	70% after 5 cycles	64
Cu(II)-AHG	24	92	Room temp.	H <sub>2</sub> O	62% after 4 cycles	63
Cu(II)-AD	48	95	Room temp.	H <sub>2</sub> O	62% after 4 cycles	63
						
CE-CD-Cu	24	96	40	H <sub>2</sub> O	6 cycles	75
						
Cu(I)@pNIPAM-VP	2	94	60	H <sub>2</sub> O	6 cycles	76
Cu(II)@pNIPAM-VP	2	91	60	H <sub>2</sub> O	6 cycles	76
Cu(II)@IPSi	24	91	Room temp.	H <sub>2</sub> O	6 cycles	76
						
Cu <sub>2</sub> O microspheres	24	95	Room temp.	H <sub>2</sub> O	Not specified	77
This work	8	96	Room temp.	H <sub>2</sub> O	87% after 6 cycles	—



significant activity, and good recyclability. In addition, the uniform dispersion of nanoparticles in the sponge-like hydrogel matrix provides a medium in which the valuable properties of the nanoparticles, including their high catalytic activity and large surface area, can be exploited.

The comparison of the synthesized chitosan/CuFe<sub>2</sub>O<sub>4</sub> nanocomposite hydrogel catalyst with other catalysts demonstrates its suitable performance under green conditions (see Table 4). This catalyst achieves a high yield of 96% at room temperature after 8 h using water as the solvent, which is both environmentally friendly and energy-efficient compared to other catalysts that require higher temperatures or organic solvents. Furthermore, its catalytic activity was maintained over six successive cycles, showing its great reusability and cost-effectiveness. The combination of high efficiency, mild reaction conditions, and sustainability indicates the novelty and potential of the green and recyclable in practical applications.

## 4. Conclusions

In this study, a novel heterogenous catalyst for the synthesis of 1,2,3-triazoles was prepared from chitosan and formaldehyde, in the presence of Cu(NO<sub>3</sub>)<sub>2</sub>·3H<sub>2</sub>O and Fe(NO<sub>3</sub>)<sub>3</sub>·9H<sub>2</sub>O, using a simple two-step process. The process involved cross-linking of chitosan with formaldehyde, followed by *in situ* preparation of CuFe<sub>2</sub>O<sub>4</sub> nanoparticles in the hydrogel network. The resulting CuFe<sub>2</sub>O<sub>4</sub> nanocomposite hydrogel was characterized by XRD and EDX analysis. DLS and HR-TEM analysis indicated that the nanoparticles have the sizes of about 5–30 nm. The catalytic ability of the nanocomposite hydrogel was studied in the synthesis of 1,2,3-triazoles and the results indicated that the nanocomposite hydrogel can act as an effective catalyst for the cycloaddition reaction. In addition, the activity of the catalyst was maintained even after six cycles. The CuFe<sub>2</sub>O<sub>4</sub> nanocomposite hydrogel can be introduced as an effective catalyst for green synthesis of triazoles, with easy synthesis, comfortable separation, and proper catalyst stability.

## Data availability

The data supporting this article have been included as part of the ESI.† Crystallographic data for the reported compound have been deposited at the Cambridge Crystallographic Data Center (CCDC-No. 2264680).

## Conflicts of interest

The authors declare that there is no conflicts of interest.

## Acknowledgements

We thank Imam Khomeini International University and the University of Zanjan for supporting this study.

## References

1 R. A. Sheldon, *ACS Sustainable Chem. Eng.*, 2018, **6**, 32–48.

- 2 M. Sajid and J. Płotka-Wasyłka, *Talanta*, 2022, **238**, 123046.
- 3 J. B. Zimmerman, P. T. Anastas, H. C. Erythropel and W. Leitner, *Science*, 2020, **367**, 397–400.
- 4 Y. Liu, J. Wang, H. Chen and D. Cheng, *Sci. Total Environ.*, 2022, **846**, 157303.
- 5 H. Nasution, H. Harahap, N. F. Dalimunthe, M. H. S. Ginting, M. Jaafar, O. O. Tan, H. K. Aruan and A. L. Herfananda, *Gels*, 2022, **8**, 568.
- 6 X. Xue, Y. Hu, S. Wang, X. Chen, Y. Jiang and J. Su, *Bioact. Mater.*, 2022, **12**, 327.
- 7 Y. Zhou, X. Dong, Y. Mi, F. Fan, Q. Xu, H. Zhao, S. Wang and Y. Long, *J. Mater. Chem. A*, 2020, **8**, 10007–10025.
- 8 H. Liu, C. Wang, C. Li, Y. Qin, Z. Wang, F. Yang, Z. Li and J. Wang, *Mater. Horiz.*, 2018, **8**, 7533–7549.
- 9 B. Tian, S. Hua, Y. Tian and J. Liu, *J. Mater. Chem.*, 2020, **8**, 10050–10064.
- 10 L. Li, S. Jia, S. Yue, C. Wang, H. Qiu, Y. Ji, M. Cao and D. Zhang, *Green Chem.*, 2024, **26**, 6404–6422.
- 11 X. N. Zhang, Q. Zheng and Z. L. Wu, *Composites, Part B*, 2022, **238**, 109895.
- 12 R. Foudazi, R. Zowada, I. Manas-Zloczower and D. L. Feke, *Langmuir*, 2023, **39**, 2092.
- 13 S. Awasthi, J. K. Gaur, M. S. Bobji and C. Srivastava, *J. Mater. Sci.*, 2022, **57**, 8041.
- 14 P. Manhas, R. Sharma, N. Wangoo, R. Saini, M. Saima, J. N. Agrewala and R. K. Sharma, *J. Mol. Liq.*, 2023, **383**, 122170.
- 15 O. Kapusta, A. Jarosz, K. Stadnik, D. A. Giannakoudakis, B. Barczyński and M. Barczak, *Int. J. Mol. Sci.*, 2023, **24**, 2191.
- 16 T. Pan, Y. Zhang, X. Qu, X. Liang and Y. Zhao, *New J. Chem.*, 2024, **48**, 7785–7798.
- 17 C. Chen, X. Yang, S.-j. Li, C. Zhang, Y.-n. Ma, Y.-x. Ma, P. Gao, S.-Z. Gao and X.-j. Huang, *Green Chem.*, 2021, **23**, 1794–1804.
- 18 S. Panja, S. Hanson and C. Wang, *ACS Appl. Mater. Interfaces*, 2020, **12**, 25276.
- 19 R. Malik, R. Saxena and S. G. Warkar, *ChemistrySelect*, 2023, **8**, e202203670.
- 20 J. Li, W. Song and F. Li, *Gels*, 2023, **9**, 239.
- 21 H. Labie and M. Blanzat, *Biomater. Sci.*, 2023, **11**, 4073–4093.
- 22 S. H. Jeong, S. Cheong, T. Y. Kim, H. Choi and S. K. Hahn, *ACS Appl. Mater. Interfaces*, 2023, **15**, 16471.
- 23 K. Thirupathi, C. J. Raorane, V. Ramkumar, S. Ulagesan, M. Santhamoorthy, V. Raj, G. S. Krishnakumar, T. T. V. Phan and S.-C. Kim, *Gels*, 2022, **9**, 35.
- 24 B. S. Kaith, A. Singh, A. K. Sharma and D. Sud, *J. Polym. Environ.*, 2021, **29**, 3827.
- 25 Y. Du and G. Feng, *Green Chem.*, 2023, **25**, 8349–8384.
- 26 P. Slavik and D. K. Smith, *Tetrahedron*, 2020, **76**, 131344.
- 27 P. Slavik, D. W. Kurka and D. K. Smith, *Chem. Sci.*, 2018, **9**, 8673.
- 28 Y. Y. Li Sip, D. W. Fox, L. R. Shultz, M. Davy, H.-S. Chung, D.-X. Antony, Y. Jung, T. Jurca and L. Zhai, *ACS Appl. Nano Mater.*, 2021, **4**, 6045.
- 29 J. Dadashi, M. A. Ghasemzadeh and M. Salavati-Niasari, *RSC Adv.*, 2022, **12**, 23481.
- 30 A. Khalil, N. Ali, A. Khan, A. M. Asiri and T. Kamal, *Int. J. Biol. Macromol.*, 2020, **164**, 2922.



- 31 C. Gao, X. Wang, S. Zhai and Q. An, *Int. J. Biol. Macromol.*, 2019, **134**, 202.
- 32 N. Maddahzadeh-Darini, S. Rezheh, M. Ghorbanloo, M. Mori, H. Yahiro and T. Mokary-Yazdeli, *New J. Chem.*, 2022, **46**, 13661.
- 33 M. Hrimla, L. Bahsis, M. R. Laamari, M. Julve and S.-E. Stiriba, *Int. J. Mol. Sci.*, 2022, **23**, 1.
- 34 L. Jia, X.-Y. Jin, L.-X. Zhao, Y. Fu and F. Ye, *J. Agric. Food Chem.*, 2022, **70**, 5499.
- 35 F. Wang, L. Zhao, F. Song, J. Wu, Q. Zhou and L. Xie, *J. Mater. Chem. B*, 2021, **9**, 3377–3388.
- 36 D. Osmaniye, N. Baltacı Bozkurt, S. Levent, G. Benli Yardımcı, B. N. Sağlık, Y. Ozkay and Z. A. Kaplancıklı, *ACS Omega*, 2023, **27**, 24573.
- 37 A. Rani, G. Singh, A. Singh, U. Maqbool, G. Kaur and J. Singh, *RSC Adv.*, 2020, **10**, 5610–5635.
- 38 C. Verma, E. E. Ebenso, M. A. Quraishi and C. M. Hussain, *Mater. Adv.*, 2021, **2**, 3806.
- 39 Y. S. Yen, J. L. Hsu, J. S. Ni and J. T. Lin, *Dyes Pigm.*, 2021, **188**, 109220.
- 40 P. Sharma, J. Rathod, A. P. Singh, P. Kumar and Y. Sasson, *Catal. Sci. Technol.*, 2018, **8**, 3246.
- 41 A. A. Rashad, K. Acharya, A. Haftl, R. Aneja, A. Dick, A. P. Holmes and I. Chaiken, *Org. Biomol. Chem.*, 2017, **15**, 7770–7782.
- 42 X. Jiang, G. Wu, W. A. Zalloum, M. E. Meuser, A. Dick, L. Sun, C.-H. Chen, D. Kang, L. Jing, R. Jia, S. Cocklin, K.-H. Lee, X. Liu and P. Zhan, *RSC Adv.*, 2019, **9**, 28961.
- 43 B. Zhang, *Eur. J. Med. Chem.*, 2019, **168**, 357.
- 44 D. R. Buckle, D. J. Outred, C. J. Rockell, H. Smith and B. A. Spicer, *J. Med. Chem.*, 1983, **26**, 251.
- 45 P. Yadav, K. Lal, A. Kumar, S. K. Guru, S. Jaglan and S. Bhushan, *Eur. J. Med. Chem.*, 2017, **126**, 944.
- 46 L. Gonnet, M. Baron and M. Baltas, *Molecules*, 2021, **26**, 5667.
- 47 V. K. Tiwari, B. B. Mishra, K. B. Mishra, N. Mishra, A. S. Singh and X. Chen, *Chem. Rev.*, 2016, **116**, 3086.
- 48 H. C. Kolb, M. G. Finn and K. B. Sharpless, *Angew. Chem., Int. Ed. Engl.*, 2001, **40**, 2004.
- 49 G. S. Reddy, L. M. Reddy, A. S. Kumar and D. B. Ramachary, *J. Org. Chem.*, 2020, **85**, 15488.
- 50 C. Huang, X. Geng, P. Zhao, Y. Zhou, X.-X. Yu, L.-S. Wang, Y.-D. Wu and A.-X. Wu, *J. Org. Chem.*, 2021, **86**, 13664.
- 51 V. V. Rostovtsev, L. G. Green, V. V. Fokin and K. B. Sharpless, *Angew. Chem., Int. Ed. Engl.*, 2002, **114**, 2708.
- 52 M. Meldal and C. W. Tornøe, *Chem. Rev.*, 2008, **108**, 2952.
- 53 F. Ajormal, R. Bikas, N. Noshiranzadeh, A. Kozakiewicz-Piekarz and T. Lis, *New J. Chem.*, 2022, **46**, 19468.
- 54 N. Z. Fantoni, A. H. El-Sagheer and T. Brown, *Chem. Rev.*, 2021, **121**, 7122.
- 55 G. S. Rani, M. Vijay and B. L. A. Prabhavathi Devi, *ChemistrySelect*, 2019, **4**, 10133.
- 56 S. Cao, Y. Liu, C. Hu, C. Wen and J.-P. Wan, *Chem. Cat. Chem.*, 2018, **10**, 5007.
- 57 H. Lee, J. K. Lee, S.-J. Min, H. Seo, Y. Lee and H. Rhee, *J. Org. Chem.*, 2018, **83**, 4805.
- 58 A. K. Agrahari, P. Bose, M. K. Jaiswal, S. Rajkhowa, A. S. Singh, S. Hotha, N. Mishra and V. K. Tiwari, *Chem. Rev.*, 2021, **121**, 7638.
- 59 N. George, G. Singh, R. Singh, G. Singh, A. Devi, H. Singh, G. Kaur and J. Singh, *Chem. Pharm.*, 2022, **30**, 100824.
- 60 S. A. Jasim, Y. Riadi, H. S. Majdi and U. S. Altimari, *RSC Adv.*, 2022, **12**, 17905.
- 61 N. Aflak, H. Ben El Ayouchia, L. Bahsis, H. Anane, M. Julve and S.-E. Stiriba, *Int. J. Mol. Sci.*, 2022, **23**, 2383.
- 62 V. Kumar, K. Lal Naveen and R. K. Tittal, *Catal. Commun.*, 2023, **176**, 106629.
- 63 L. Bahsis, E.-H. Ablouh, H. Anane, M. Taourirte, M. Julve and S.-E. Stiriba, *RSC Adv.*, 2020, **10**, 32821–32832.
- 64 J. F. Souza, G. P. Costa, R. Luque, D. Alves and A. R. Fajardo, *Catal. Sci. Technol.*, 2019, **9**, 136.
- 65 M. C. Pellá, M. K. Lima-Tenório, E. T. Tenório-Neto, M. R. Guilherme, E. C. Muniz and A. F. Rubira, *Carbohydr. Polym.*, 2018, **96**, 233–245.
- 66 M. Sadeghi, F. Hanifpour, R. Taheri, H. Javadian and M. Ghasemi, *Process Saf. Environ. Prot.*, 2016, **102**, 119.
- 67 S. Mallakpour and E. Khadem, *Int. J. Biol. Macromol.*, 2018, **120**, 1451.
- 68 Y. Chen, Q. Duan, L. Yu and F. Xie, *Carbohydr. Polym.*, 2021, **272**, 118522.
- 69 N. Li and R. Bai, *Ind. Eng. Chem. Res.*, 2005, **44**, 6692.
- 70 R. Bikas, F. Ajormal, N. Noshiranzadeh, M. Emami and A. Kozakiewicz, *Appl. Organomet. Chem.*, 2020, **34**, e5826.
- 71 M. Emami, R. Bikas, N. Noshiranzadeh, A. Kozakiewicz and T. Lis, *ACS Omega*, 2020, **5**, 13344.
- 72 B. Sarmah, B. Satpati and R. Srivastava, *RSC Adv.*, 2016, **6**, 87066.
- 73 F. Alonso, Y. Moglie, G. Radivoy and M. Yus, *J. Org. Chem.*, 2011, **76**, 8394.
- 74 S. J. Saghanezhad, M. M. Buhamidi, S. Ebadi, N. Taheri and S. Sayyahi, *React. Kinet. Mech. Catal.*, 2021, **133**, 897.
- 75 F. Liu, X. Liu and Q. Fu, *Cellulose*, 2023, **30**, 953–971.
- 76 M. Lim, H. Lee, M. Kang, W. Yoo and H. Rhee, *RSC Adv.*, 2018, **8**, 6152–6159.
- 77 R. Rai, S. Saha, S. Ravi and A. Abbas, *Asian J. Chem.*, 2024, **36**, 1506–1510.

